ROZPRAWY INŻYNIERSKIE • ENGINEERING TRANSACTIONS • 26, 4, 619-643, 1978
Polska Akademia Nauk • Instytut Podstawowych Problemów Techniki

NUMERICAL ANALYSIS OF COMPATIBLE FINITE ELEMENTS OF DIFFERENT ORDER IN TWO-DIMENSIONAL PROBLEMS OF ELASTICITY (*)

F. BRAGA, G. REGA and F. VESTRONI (ROMA)

A large number of compatible finite element models for plane elasticity problems has been presented in the last decade. On the contrary, the number of studies so far carried out regarding the evaluation of the efficiency of different elements is small. This paper is mainly concerned with the comparison of the behaviour of compatible triangular elements of different order. Such a comparison regards mainly the results associated with *LST* and *QST* elements for different values of the number of degrees of freedom in the analysis of problems for which analytical solutions are available. Attention is focused separately on displacement and stress fields by analysing the convergence of the elements as well as the global and local approximation. A numerical analysis is also performed in order to compare the efficiency of two methods suited for encompassing lack of uniqueness of stress nodal values, as usually encountered in the compatible formulation, i.e. the simple average and the method based on the theory of conjugate approximations.

1. Introduction

A large number of f.e. models for the analysis of elasticity problems has been proposed in the last decades. These models differ both in the variational principle from which they originate and in the features of the element, such as shape, interpolation function and types of nodal parameters [1, 6].

On the contrary, the number of studies so far presented regarding the comparison of different elements in the analysis of a definite elastic continuum is rather small and some difficulties are encountered for their adequate use in structural applications. The question has been pointed out by some recent studies regarding the problems arising in the domain discretization through f.e. and the optimization of various steps of the procedure [14, 15, 16].

In this paper the behaviour of compatible triangular elements is discussed in the analysis of plane stress and strain problems.

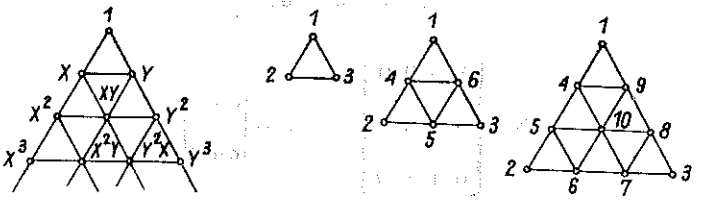

Fig. 1.

(*) Presented at the XIX-th Polish Solid Mechanics Conference Ruciane-Piaski, September 7–16, 1977.

Reference is made to the first three elements (*CST*, *LST*, *QST*) of the Lagrangian family which are generated in sequence according to Fig. 1 [8, 9, 11]. It is common knowledge that these are conforming elements in which the displacement field $\mathbf{u}$, of different order for each element, is described by the nodal parameters $\mathbf{u}_e^*$ which are the independent variables of the procedure. The relating interpolation functions are given in the Appendix.

The comparison of the various elements is carried out by analysing both the convergence properties and the global and local approximation of solutions obtained with the same number of degrees of freedom. Attention is focused on the behaviour of higher order elements.

The interpretation of stress results, which are discontinuous in compatible models, is accomplished using the method proposed by ODEN *et al*, [12, 13]. This method is based on the theory of conjugate approximation and has been previously [17] developed with reference to the elements considered in this paper. A feature of this method is that it gives a continuous stress field all over the domain. In this paper stresses obtained by Oden's method are compared with those resulting from the simple average, at each node, of the stresses for the elements incident on that node.

The numerical analysis has been processed by a computer algorithm, the list and operational features of which are furnished in Ref. [17]; such an algorithm has been expressly implemented to carry out the comparison analysis.

2. COMPATIBLE FINITE ELEMENTS

The formulation of a plane elastic problem through compatible f.e. is based on the minimization of the total potential energy functional which may be written as (1)

$$\Pi_p = \sum_e \left[\int_{V_e} \left(\frac{1}{2} \boldsymbol{\epsilon}^T \mathbf{E} \boldsymbol{\epsilon} - \mathbf{u}^T \mathbf{p} \right) dV - \int_{S_{fe}} \mathbf{u}^T \bar{\mathbf{f}} \, dS \right] \tag{2.1}$$

for a continuum discretized in a finite number of elements. In Eq. (2.1) $\boldsymbol{\epsilon}^T = \{\varepsilon_x, \varepsilon_y, \gamma_{xy}\}$ strain vector, $\mathbf{E}$ elastic constant matrix, $\mathbf{u}^T = \{u_x, u_y\}$ displacement vector, $\mathbf{p}^T = \{p_x, p_y\}$ prescribed body force vector, $\bar{\mathbf{f}}^T = \{\bar{f}_x, \bar{f}_y\}$ prescribed surface force vector, V_e element volume, S_{fe} portion of element boundary surface over which the forces $\bar{\mathbf{f}}$ are prescribed.

In applying the principle of minimum potential energy, strain field is written in terms of the displacement $\mathbf{u}$ (1):

$$\boldsymbol{\epsilon} = \mathbf{T} \rhd \mathbf{d}_c \lhd \mathbf{u}, \tag{2.2}$$

where (2)

$$\mathbf{T} = \begin{bmatrix} 1 & 0 & 0 & 0 \\ 0 & 0 & 0 & 1 \\ 0 & 1 & 1 & 0 \end{bmatrix}, \qquad \mathbf{d}_c = \begin{Bmatrix} \partial/\partial x \\ \partial/\partial y \end{Bmatrix}.$$

(1) Matrices and vectors are respectively denoted with a bold face capital and small letters.

(2) The operator $\rhd$ is defined as follows. Let $\mathbf{A}$ be a matrix of size $(n \times kp)$ that can be partitioned in the K matrices $\mathbf{A}_i$ $(n \times p)$: $\mathbf{A} = [\mathbf{A}_1 \, \mathbf{A}_2 \ldots \mathbf{A}_k]$ and let $\mathbf{B}$ be a matrix of size $(p \times m)$. Matrix $\mathbf{C}$ is

In each element e the displacement $\mathbf{u}$ is represented approximately in terms of generalized parameters $\mathbf{u}_e^* = \{u_x^* \; u_y^*\}$ through the following relationship:

$$\mathbf{u} = \mathbf{n}^T \lhd \mathbf{u}_e^*, \tag{2.3}$$

where $\mathbf{n}^T = \{n_1 \; n_2, \ldots, n_n\}$ is the vector of interpolation functions for the n-node element. The parameters $\mathbf{u}_e^*$ are the nodal displacements; the interpolation functions must be such as to assure the compatibility of displacement for two neighbouring elements when these have the same nodal values on the common side.

The Lagrangian elements considered in this paper have a number of nodes sufficient to determine the coefficients of a complete polynomial of the order $\mathbf{h}$, which defines the element and such as to assure the requested compatibility; therefore, the relating interpolation functions satisfy the above-mentioned condition [3]. From Eqs. (2.2) and (2.3) the element strain field is obtained in terms of the generalized displacement $\mathbf{u}_e^*$:

$$\boldsymbol{\epsilon} = \mathbf{D}\mathbf{u}_e^*, \tag{2.4}$$

where, taking account of the relationships (a) and (b) presented in the Appendix, there results

$$\mathbf{D} = \mathbf{T} \rhd \mathbf{J}^{-1} \mathbf{d}_l \mathbf{l}_u^T \mathbf{B}^T.$$

By substituting the expressions (2.3) and (2.4) in Eq. (2.1), the functional can be written as follows:

$$\Pi_p = \sum_e \left(\frac{1}{2} \mathbf{u}_e^{*T} \mathbf{K}_e \mathbf{u}_e^{*} - \mathbf{u}_e^{*T} \bar{\mathbf{q}}_e \right), \tag{2.5}$$

where

$$\mathbf{K}_e = \int_{V_e} \mathbf{D}^T \mathbf{E} \mathbf{D} \, dV,$$

$$\bar{\mathbf{q}}_e = \int_{V_e} \mathbf{n} \lhd \mathbf{p} \, dV + \int_{S_{fe}} \mathbf{n} \lhd \bar{\mathbf{f}} \, dS$$

are respectively the element stiffness matrix and the vector of equivalent nodal forces. Explicitly, this results in

$$\mathbf{K}_e = \int_{V_e} \mathbf{B} (\mathbf{d}_l \mathbf{l}_u^T)^T \mathbf{J}^{-1} \lhd \mathbf{T}^T \mathbf{E} \mathbf{T} \rhd \mathbf{J}^{-1} \mathbf{d}_l \mathbf{l}_u^T \mathbf{B}^T \, dV = \int_{V_e} \mathbf{G} \lhd \mathbf{H} \rhd \mathbf{G}^T \, dV. \tag{2.6}$$

---

defined by the following relationship: $\mathbf{C} = \mathbf{A} \rhd \mathbf{B}$. It has size $(n \times km)$ and is expressly given by the equation $\mathbf{C} = [\mathbf{A}_1 \mathbf{B}, \mathbf{A}_2 \mathbf{B}, \ldots, \mathbf{A}_k \mathbf{B}]$. It can be seen that there results $\rhd^T = \lhd$. A more detailed picture of the properties of the operator is furnished in Ref. [17]

[3] The expressions of interpolation functions are reported in the Appendix; a more detailed picture of the elements considered in this paper, together with the numerical expressions of their matrices, is reported in Ref. [17].

Suitably partitioning the matrices of Eq. (2.6), it follows that

$$(2.6)' \qquad \mathbf{K}_e = \int_{V_e} [\mathbf{G}_1 \,\vdots\, \mathbf{G}_2] \lhd \left[\begin{array}{c:c:c:c} \alpha & 0 & 0 & \beta \\ 0 & \gamma & \gamma & 0 \\ \hdashline 0 & \gamma & \gamma & 0 \\ \beta & 0 & 0 & \alpha \end{array}\right] \rhd \left[\begin{array}{c} \mathbf{G}_1^T \\ \hdashline \mathbf{G}_2^T \end{array}\right] dV,$$

where the elastic constants α, β, γ are, respectively

$$\frac{E(1-\nu)}{(1+\nu)(1-2\nu)}, \quad \frac{E\nu}{(1+\nu)(1-2\nu)}, \quad \frac{E}{2(1+\nu)},$$

for plane strain and

$$\frac{E}{1-\nu^2}, \quad \frac{E\nu}{1-\nu^2}, \quad \frac{E}{2(1+\nu)},$$

for plane stress, and

$$\mathbf{G}_1 = \frac{1}{2A}\left(y_{23}\,\mathbf{B}\frac{\partial}{\partial L_1}\mathbf{l}_u + y_{31}\,\mathbf{B}\frac{\partial}{\partial L_2}\mathbf{l}_u\right),$$

$$\mathbf{G}_2 = \frac{1}{2A}\left(x_{32}\,\mathbf{B}\frac{\partial}{\partial L_1}\mathbf{l}_u + x_{13}\,\mathbf{B}\frac{\partial}{\partial L_2}\mathbf{l}_u\right).$$

By developing Eq. (2.6), the final result is

$$\mathbf{K}_e = \left[\begin{array}{c:c} \alpha\,\mathbf{K}_{11} + \gamma\,\mathbf{K}_{22} & \gamma\,\mathbf{K}_{12}^T + \beta\,\mathbf{K}_{12} \\ \hdashline \gamma\,\mathbf{K}_{12} + \beta\,\mathbf{K}_{12}^T & \gamma\,\mathbf{K}_{11} + \alpha\,\mathbf{K}_{22} \end{array}\right],$$

where

$$\mathbf{K}_{ij} = \int_{V_e} \mathbf{G}_i\,\mathbf{G}_j^T\,dV.$$

As far as the nodal forces are concerned, it expressly follows that

$$\bar{\mathbf{q}}_e = \int_{V_e} \mathbf{B}\mathbf{l}_u \lhd \begin{Bmatrix} p_x \\ p_y \end{Bmatrix} dV + \int_{S_{fe}} \mathbf{B}\mathbf{l}_u \lhd \begin{Bmatrix} \bar{\mathbf{f}}_x \\ \bar{\mathbf{f}}_y \end{Bmatrix} dS.$$

If $\mathbf{s}^T = \{\mathbf{s}_x^T\ \mathbf{s}_y^T\}$ is the vector of generalized displacements for the N nodes of the whole domain, the element nodal displacements $\mathbf{u}_e^*$ can be obtained through the Boolean matrices $\mathbf{\Omega}_e\,(n \times N)$:

$$\mathbf{u}_e^* = \mathbf{\Omega}_e \lhd \mathbf{s}.$$

The functional Π_p can thus be written as

$$(2.7) \qquad \Pi_p = \frac{1}{2}\,\mathbf{s}^T\mathbf{K}\mathbf{s} - \mathbf{s}^T\bar{\mathbf{q}},$$

where

$$\mathbf{K}=\sum_e \boldsymbol{\Omega}_e^T \lhd \mathbf{K}_e \rhd \boldsymbol{\Omega}_e ,$$

$$\bar{\mathbf{q}}=\sum_e \boldsymbol{\Omega}_e^T \lhd \bar{\mathbf{q}}_e$$

are respectively the stiffness matrix of the assembled structure and the vector of generalized nodal forces.

If $\bar{\mathbf{s}}_2$ are the displacement components prescribed in the boundary portion S_u and $\mathbf{q}_2$ are the corresponding unknown components of the nodal forces vector, the functional can be partitioned as follows:

$$\Pi_p=\frac{1}{2}\{\mathbf{s}_1^T \bar{\mathbf{s}}_2^T\}\begin{bmatrix}\mathbf{K}_{11} & \mathbf{K}_{12}\\ \mathbf{K}_{12}^T & \mathbf{K}_{22}\end{bmatrix}\begin{Bmatrix}\mathbf{s}_1\\ \mathbf{s}_2\end{Bmatrix}-\{\mathbf{s}_1^T \bar{\mathbf{s}}_2^T\}\begin{Bmatrix}\bar{\mathbf{q}}_1\\ \mathbf{q}_2\end{Bmatrix},$$

where $\mathbf{s}_1$ are the unknown displacement components and $\bar{\mathbf{q}}_1$ are the prescribed loads. The stationarity condition $\delta\pi_p=0$ will yield

$$\mathbf{K}_{11}\mathbf{s}_1=\bar{\mathbf{q}}_1-\mathbf{K}_{12}\bar{\mathbf{s}}_2 .$$

The element displacements $\mathbf{u}_e^*$ can then be easily obtained and element stresses are finally calculated through Eq. (2.4):

$$\boldsymbol{\sigma}_e=\mathbf{E}\mathbf{D}\mathbf{u}_e^*=\mathbf{S}_e\mathbf{u}_e^* , \tag{2.8}$$

where $\mathbf{S}_e=\mathbf{E}\mathbf{T}\rhd\mathbf{G}^T$ is the stress matrix.

3. Results obtained for displacement field with the different elements

In the discretization of elastic continua via compatible f.e., displacements $\mathbf{u}$ are the fundamental quantities; stresses $\boldsymbol{\sigma}$ are obtained from element by element displacements.

It is suitable to analyse separately the results obtained with elements of different order for displacement and stress fields. Firstly, displacements are considered; in fact, since they are the independent parameters of the procedure, they result in a more meaningful way in order to evaluate the performance of the numerical method. Afterwards, the stress field is analysed; its approximation is connected, besides with displacements variables, also with the procedure through which univocal values are obtained.

The comparison of the f.e. solutions obtained for a definite problem is usually carried out — in the literature — with reference to the total number of d.o.f. of the discretized structure. In the present paper too this parameter, which is representative enough of the calculation global onerousness, has been assumed (4).

(4) Here it must be noted that the global calculation onerousness chiefly depends on the size of the equation system that is equal to the total number of d.o.f. However, it also depends on other parameters connected to the type of element such as the bandwith of the stiffness matrix which has a considerable influence on core storage and solution time, and the data generation and input time.

Structural problems for which analytical solutions are known have been considered; the error of numerical solutions has been evaluated referring to the former ones. The major part of the comparison has been carried out considering a uniformly loaded simple beam. In this case displacement boundary conditions can be prescribed on the discretized structure according to the analytical solution. On the contrary, considering a cantilever beam as more often examined in the literature (Refs. [9, 10, 11]) the boundary condition on the rotation can be prescribed only in an approximate way on the discrete model. Two cases have been considered for the simple beam (Fig. 2), they are defined by the two values of ratio $L/2H$, respectively, equal to 1 and 4, afterwards indicated as $B1$ and $B4$. This study has been carried out to analyse the behaviour of the various elements in problems with different geometry of the domain and different ratios of stress components. A square plate with a circular hole subjected to traction on two sides (Fig. 3) has also been studied. The purpose of this analysis is to evaluate the approximation obtainable in the analysis of stress concentration with different order elements (5).

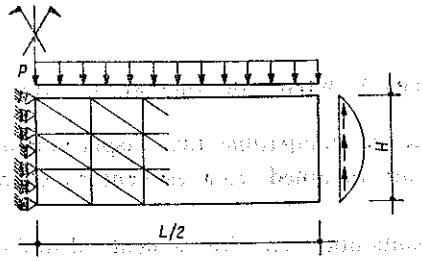

FIG. 2. Uniformly loaded simply supported beam (cases $B1$, $B4$).

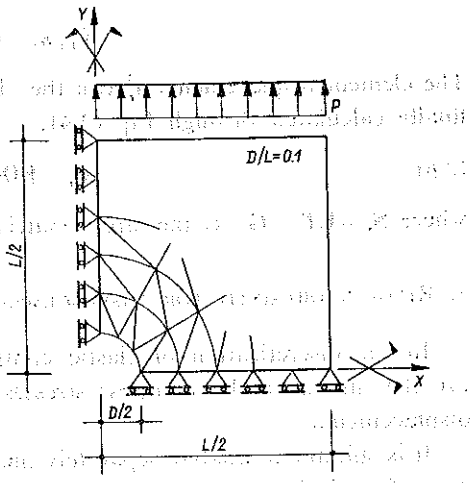

FIG. 3. Square plate with circular hole.

Since the discretization into triangular elements does not allow to represent exactly the circular boundary of the hole, a definite polygonal boundary (32 sides) has been considered. The error is calculated with reference to an „exact" solution obtained numerically using a very refined mesh.

Convergence properties to the exact solution have a considerable importance in numerical methods. Asymptotic convergence is guaranteed for the compatible elements

(5) The results of the numerical applications are expressed by units Kg, cm and refer to the following data:
simple beam: $H=600$, $s=1$, $p=10$, $E=2.1\times10^6$,
square plate: $L=10$, $s=1$, $p=10$, $E=2.1\times10^6$.

considered in this paper (Refs. [3, 4]). From the practical point of view, however, it is interesting to examine chiefly the rate of convergence of numerical solutions which strongly influence the operational performance of the method.

The error curve obtained for the displacement component u_y in case $B4$ solved through CST elements is shown in Fig. 4 in terms of the total number of nodes N of the discretized structure. From a general point of view it represents the behaviour of all f.e. solutions and gives the opportunity of some premises.

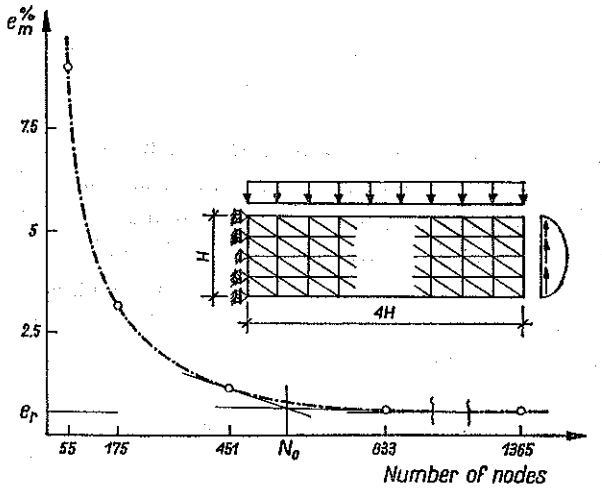

FIG. 4. Convergence properties of f.e. solutions (case $B4$, displacement component u_y).

Figure 4 shows that the solution error is almost constant over a wide N range even though it decreases as the number of nodes increases up to the value N_r, beyond which the roundoff errors prevail. Therefore, two circumstances occur: first, a definite residual value of the error exists and it cannot be eliminated by mesh refinement, second, there is a number of d.o.f. beyond which the error decrease is unimportant as regards the calculation onerousness. The performance of the various elements must be then analyzed referring to two quantities: minimum residual error e_r and optimal value N_0 of the number of nodes.

In the literature the analysis of numerical solutions is usually performed referring to the error relevant to a displacement of a particular point of the structure (Refs. [5, 10]). In more recent studies, however, reference is made to the approximation obtainable for the potential energy functional of the problem (Refs. [15, 16]).

In some cases the first procedure is representative enough of the solution behaviour on the whole: e.g. the case of the error relevant to midspan deflection in problem $B4$. This is different in a structural problem where the components of the displacement field have comparable values as in case $B1$.

On the contrary, the total potential energy represents a unitary criterion for the evaluation of numerical solutions obtained for different structural problems and provides an error related to the whole domain. In this paper, however, refer-

rence is made to the global error of the components of displacement and stress in order to analyse the behaviour of the various elements in the approximation of those quantities which are interesting from the structural point of view. The mean error of the single component calculated with respect to its maximum value is defined as follows (6)

$$e_m = \frac{1}{N} \sum_{1}^{N} i \frac{|x_i - \bar{x}_i|}{x_{\max}}. \tag{3.1}$$

In Eq. (3.1) x_i and $\bar{x}_i$ are respectively the calculated and the exact values of the component x in the node i and N is the total number of nodes.

The diagrams of the mean error e_m of the displacement components u_x, u_y relevant to *LST* and *QST* elements are reported in Fig. 5 in terms of the number N; the corresponding diagrams for case *B*4 are shown in Fig. 6.

Two considerations arise immediately from the analysis of these two figures: first, the error decreases in a very regular way the more the number of d.o.f. increases, second, the higher order elements have lower values of e_r and N_0. Therefore, solution accuracy and rate of convergence with mesh refinement are higher for *QST* elements. This latter feature is pointed out by the greater values of tangent slope to the relevant curve for a given error. Moreover, the convergence rate of *QST* elements is very high up to the low error values; on the contrary, the *LST* one decreases smoothly as the solution approaches the exact one. So, even though both elements have a comparable residual error, *QST* convergence curves exhibit better behaviour in the lower values range of the number of d.o.f. The error curve of *CST* elements is not shown in Figs. 5 and 6 even though it has similar general features; the values of e_r and N_0 are in this case considerably higher than those connected with *LST* and *QST* error curves (see Fig. 7). Accordingly, the comparison will be chiefly carried out between *LST* and *QST* elements.

The error curves (e_m, N) previously examined show the global approximation of the solution obtained with the various elements to the exact one; it is interesting however, to examine the local approximation, too. Accordingly, histograms of errors of horizontal and vertical displacements in mesh nodes are furnished for cases *B*1, *B*4 in Fig. 8; the errors are referred to the local values of the components. The figure indicates low values of local error in a larger number of points for higher order elements. Their histograms are more gathered around the vertical axis than those of lower order elements.

In addition, it can be noted (Fig. 8c, d) that while both components of displacement are well-behaved in *QST* elements, the *LST* ones penalize the lower quantities

(6) The error expression (3.1) is a weighted mean of errors $x_i - \bar{x}_i/\bar{x}_i$ connected with the N mesh nodes and affected with the multipliers $\bar{p}_i = \bar{x}_i/\bar{x}_{\max}$ such as to emphasize the errors relevant to maximum values of the quantity. This choice is due to the importance that the approximation of such values has in the analysis of structural behaviour. Assuming that $\bar{x}_{\max} \simeq x_{\max}$, we obtain

$$e_m = \sum_{1}^{N} \frac{|x_i - \bar{x}_i|}{\bar{x}_i} \bar{x}_i / x_{\max}$$

and Eq. (3.1) follows.

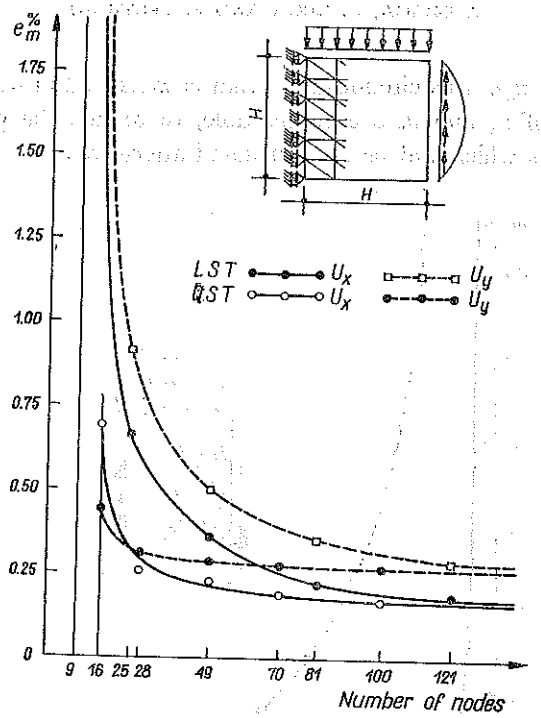

FIG. 5. $B1$: error curves of displacement components u_x, u_y with *LST*, *QST* elements.

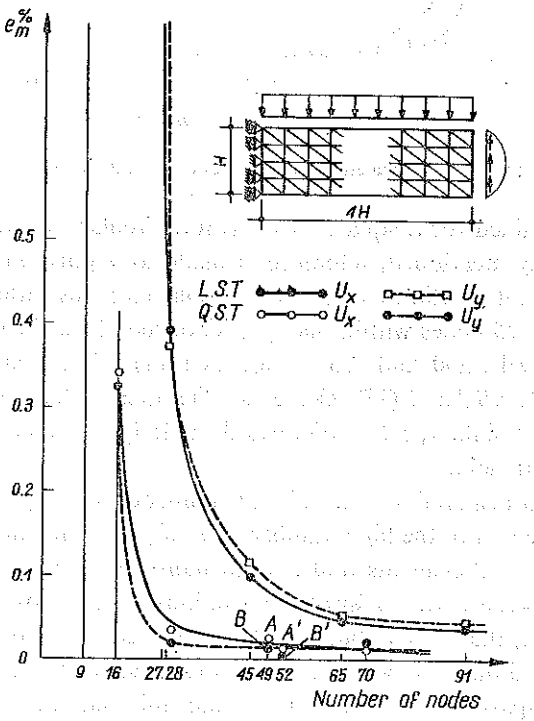

FIG. 6. $B4$: error curves of displacement components u_x, u_y with *LST*, *QST* elements.

(see the component u_x). This circumstance, that is weakened in case $B1$ (Fig. 8a, b) where the values of u_x and u_y are comparable, represents the general behaviour of the two elements which will be seen in detail afterwards.

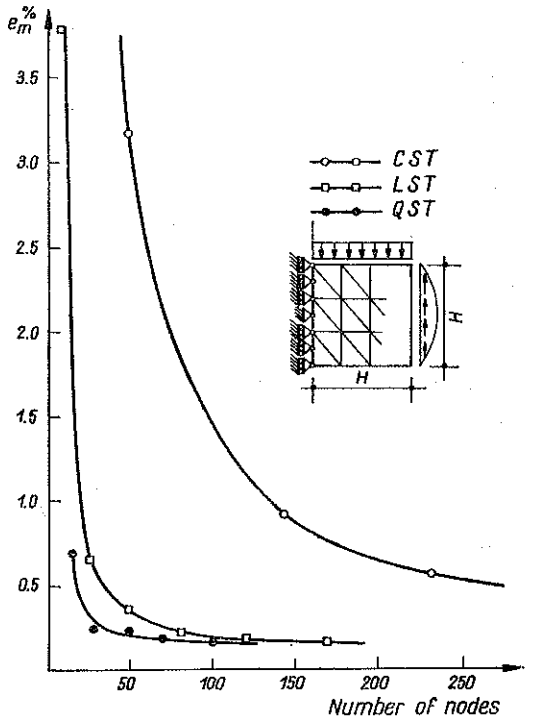

FIG. 7. $B1$: error curves of displacement component u_x with the three different elements.

The results obtained for a square plate with a circular hole are also considered (Fig. 9). As already mentioned, reference is made to a polygonal hole of 32 sides assuming a numerical solution as the comparison one; this latter is obtained with *QST* elements and 775 nodes within one quarter of the plate. Two meshes are considered with, respectively, 250 and 475 nodes, each one being used in order to obtain solutions with *CST*, *LST* and *QST* elements. The hole ovalization described by the values u_x, u_y of the points A, B (see Fig. 9 and Table 1) is assumed as representative of the displacement field.

The solutions corresponding to the higher number of nodes (475) are well-behaved enough. Taking account of the high number of d.o.f., the differences are unimportant between *QST* and *LST* elements and a little more remarkable for *CST* elements, as it occurs in the beam case. As far as the solutions with the lower number of nodes (250) are concerned, the results obtained with the three elements considerably differ one from another. Unlike the beam case, a better behaviour of *QST* elements comes out, even in comparison with *LTS* elements; this circumstance is connected with the wider capability of higher order elements of approximating complex stress fields.

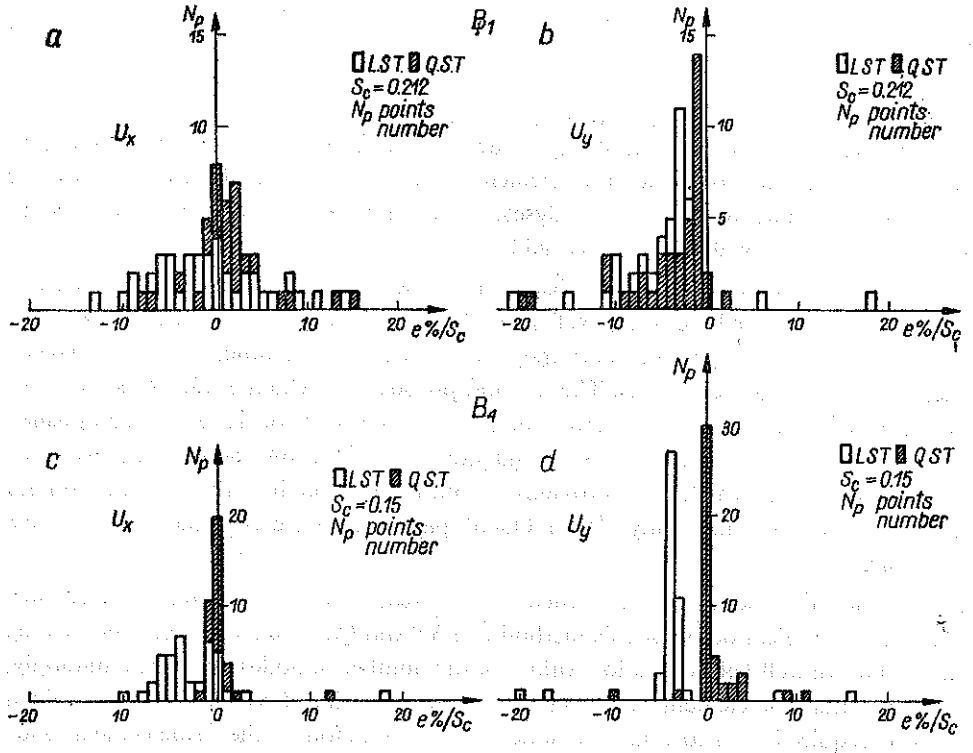

FIG. 8. Error histograms of components u_x, u_y, for cases $B1$ (a, b) and $B4$ (c, d) 49 nodes mesh.

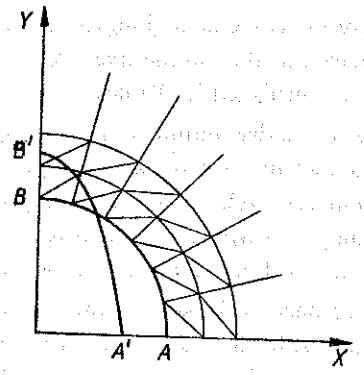

FIG. 9.

Table 1. Square plate: hole ovalization.

	250C	250L	250Q	475C	475L	475Q	775Q
$u_y^B \times 10^5$	+.6814	+.7025	+.7243	+.7189	+.7304	+.7325	+.7342
$u_x^A \times 10^5$	−.2261	−.2348	−.2484	−.2501	−.2550	−.2552	−.2556

4. Interpretation of stress results

Stresses obtained through compatible elements, as examined in this paper, are discontinuous along the inter-element boundaries; since these quantities are notably important in structural analyses, an interpolation method must be used to obtain a univocally defined stress field.

Stress interpolation has been discussed by several authors in the last decade. Most of the suggested methods (Ref. [7]) rely on the average procedure of the nodal values relative to single elements; they differ one from another in the weighting factors assigned to such values. The method proposed by Oden et al. (Refs. [12, 13]) is quite different from the previous ones. Stress interpolation is here accomplished using an approach based on the conjugate approximation theory that accounts for the whole stress field and provides a continuous function all over the domain instead of nodal values only (7). In Oden's paper reference is made only to *CST* elements.

On the other hand, as the element size increases, stress discontinuities become higher; the application of Oden's method to *LST* and *QST* elements seems interesting since they are well-behaved at low values of the number of nodes or, correspondingly, at high values of element size. On the contrary, using *CST* elements, a refined mesh is required even to obtain a suitable approximation of the displacement field; therefore, in this case element size is quite small.

Oden's method involves the inversion of a matrix the order of which is equal to the total number of nodes; it is therefore quite onerous. In order to analyse the convenience of its application, a large numerical investigation has been performed using the three types of elements. Attention is focused on the values obtained for stresses in some nodes where many elements join together. For such nodes the values relative to the different elements, the simple average one (σ_A), the Oden one (σ_O) and the "exact" one (σ_E) are furnished in Tables 2÷6.

It can be noticed that the stress discontinuity is quite slight for structural examples with a number of d.o.f. sufficient to represent adequately the actual stress state (see the patterns of Fig. 10 in case *B*1). In this respect, *QST* elements are particularly efficient; their solutions, compared with those of lower order elements, which are of lower size for a given number of d.o.f., do not present major discontinuities.

Even though these latter become larger, as for lower order elements when the number of d.o.f. decreases (Tables 3 and 5) the errors are comparable and opposite in sign as regards the "exact" stress value, so that the simple average gives stresses with small errors, which are in any case lower than discontinuities themselves.

The results obtained by means of Oden's procedure are nearly coincident with those furnished by the simple average. This circumstance occurs both when these

(7) A synthesis of Oden's method, considering the elements discussed in this paper, is presented in Ref. [17] together with the numerical expressions of the matrices needed to determine the stresses nodal values.

latter results have a good accuracy, as in most cases, and when errors are remarkable. Indeed it always occurs that σ_0 is nearer to σ_A than to the exact value and sometimes it is further than σ_A (see Tables 3 and 4).

Table 2. *B1-49QS*-**Element nodal stresses, "Exact" stress (E), simple average stress (A), Oden stress (O).**

Node	σ_x	σ_y	τ_{xy}
28	−21.40	−10.39	.037
	−21.22	−10.51	−.332
	−19.65	−9.87	.172
E	−21.20	−10.00	.000
A	−20.76	−10.26	−.040
O	−20.87	−10.24	.000
27	−12.13	−9.09	5.08
	−12.48	−9.20	5.08
E	−12.28	−9.26	5.00
A	−12.31	−9.15	5.06
O	−12.27	−9.13	5.05
25	.008	−5.14	8.96
	.044	−5.02	9.18
	−.525	−4.85	9.00
	−.091	−4.72	8.81
	−.065	−4.63	8.72
	.295	−5.05	8.62
E	.000	−5.00	9.00
A	−.056	−4.90	8.88
O	−.086	−4.91	8.91
46	−.987	−5.07	14.85
	−.035	−5.17	14.97
	.089	−4.75	14.78
E	.000	−5.00	15.00
A	−.311	−5.00	14.87
O	−.343	−5.01	14.84

We have similar observations when we consider stress results near the square plate hole. For a given element, discontinuities increase as the number of d.o.f. decreases (see examples 475Q — 250Q in Table 6); moreover, under the same number

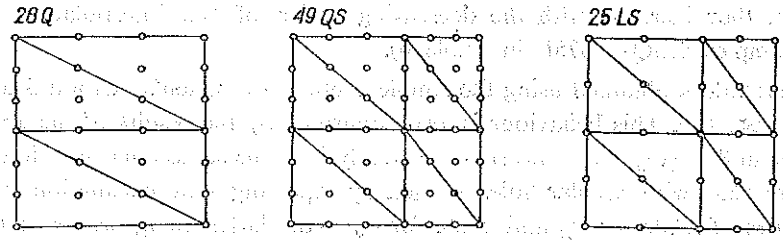

FIG. 10. Mesh patterns for case *B1*.

Table 3. *B*1-25*LS*- **Element nodal stresses, "Exact" stress (E), simple average stress (A), Oden stress (O).**

Node	σ_x	σ_y	τ_{xy}	
5	−26.62	−11.67	.13	
	−33.03	−10.54	−2.01	
	−32.00	−10.00	.00	E
	−29.83	−11.11	−.94	A
	−29.36	−10.84	−.31	O
13	−.15	−4.45	10.40	
	−.41	−5.30	7.62	
	6.32	−4.48	10.33	
	.05	−6.36	10.40	
	.03	−6.43	9.77	
	1.87	−3.84	11.08	
	.00	−5.00	9.00	E
	1.29	−5.14	9.95	A
	1.48	−5.03	9.88	O
23	5.90	−5.68	16.33	
	.75	−7.10	14.69	
	.11	−4.23	17.14	
	.00	−5.00	15.00	E
	1.75	−5.67	16.05	A
	1.34	−5.78	15.98	O

Table 4. *B*1-28*Q*- **Element nodal stresses, "Exact" stress (E), simple average stress (A), Oden stress (O).**

Node	σ_x	σ_y	τ_{xy}	
7	−32.99	−10.36	−.71	
	−33.02	−10.83	−.71	
	−32.00	−10.00	.00	E
	−33.00	−10.60	−.71	A
	−32.99	−10.55	.53	O
25	.047	−4.56	14.96	
	−.160	−5.23	14.55	
	.380	−4.80	14.91	
	.000	−5.00	15.00	E
	.089	−4.86	14.81	A
	.110	−4.84	14.82	O

of d.o.f. they increase with the decreasing order of the interpolation function (see examples 475Q — 475L in Table 6).

Stress values obtained using the simple average and Oden's method draw closer in this case, too. This behaviour is also confirmed by the results of the application reported in Ref. [13], just concerning the analysis of the stress concentration factor in a square plate with circular hole. In fact, by repeating that calculation (Fig. 11a), the values of 28.06 for σ_A and 29.84 for σ_0 — the latter being nearer to the exact one — are obtained for the component σ_y at hole boundary near the horizontal

Table 5. *B4-55C-* **Element nodal stresses, "Exact" stress (E), simple average stress (A), Oden stress (O).**

ELEM	σ_x	σ_y	τ_{xy}	Node 18
19	6.5126	22.672	63.684	
20	−176.51	−32.671	−38.835	
22	−8.6312	−27.807	−37.912	
27	7.0385	22.394	65.877	
29	166.17	24.034	66.160	
30	−7.2284	−25.162	−29.700	
E	0.000	−5.00	+18.000	
A	−2.4416	−2.7577	14.879	
O	−1.8830	−3.2384	14.879	

ELEM	σ_x	σ_y	τ_{xy}	Node 16
18	−345.77	−37.565	−46.127	
25	−149.23	21.396	58.894	
26	−325.34	−36.286	−39.996	
E	−438.80	−10.00	0.000	
A	−273.45	−17.485	−9.0762	
O	−333.21	−25.262	−23.942	

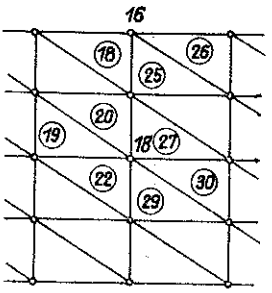

axis. From this result a better accuracy of Oden's method is obtained. The difference between σ_A and σ_0, which occurs only in boundary nodes, is, however, quite fictitious; in fact, the values 28.06 for σ_A must be placed at the centre of the boundary element, being *CST* elements. The value 30.26, that is nearer to σ_0, would be otherwise obtained by calculating the boundary stress value through linear extrapolation of the results in points *B* and *H* (Fig. 11b).

For inside nodes the average of stresses relative to neighbouring elements gives exactly the values corresponding to the nodal points. The comparis onwith the anal-

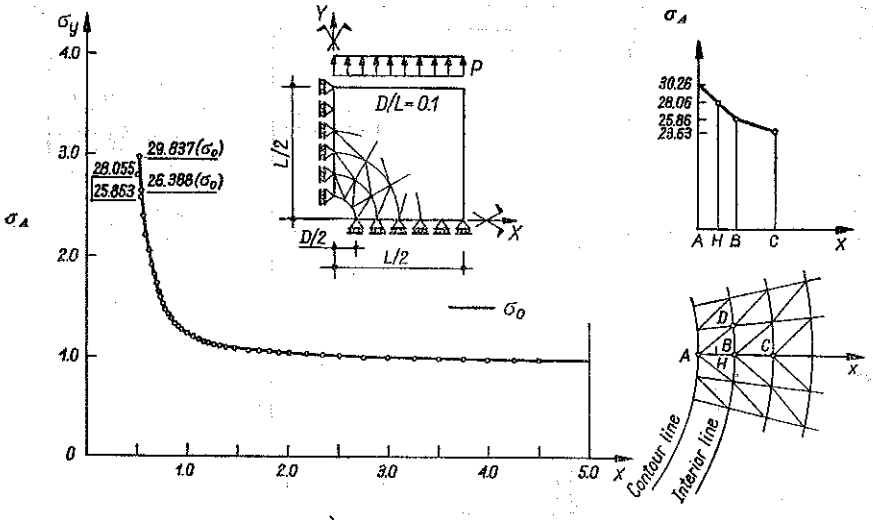

FIG. 11. Square plate (435 nodes mesh). σ_y component along x axis.

Table 6. Square plate: element nodal stresses, simple average stress (A), Oden stress (O) for the examples 475Q, 475C, 250Q.

Node *A*

EL	σ_x	σ_y	τ_{xy}
1	−0.03569	−33.604	1.3294
2	−0.79699	−31.197	−0.27885
0	−0.55465	−32.572	0.48006
M	−0.41634	−32.600	0.52529

Node *A*

EL	σ_x	σ_y	τ_{xy}
2	−1.6944	−31.614	1.7674
1	−1.3734	−27.250	−0.39916
0	−1.5650	−30.963	0.23356
M	−1.4339	−29.332	0.68412

Node *A*

EL	σ_x	σ_y	τ_{xy}
1	−0.40122	−32.05	0.43586
2	−0.76327	−29.116	0.23101
0	−0.42045	−30.447	0.25428
M	−0.58224	−30.583	0.33344

Node *B*

EL	σ_x	σ_y	τ_{xy}
1	−2.9404	−21.990	2.3376
2	−3.2299	−21.986	2.3310
3	−2.9387	−21.901	2.3310
4	−2.8412	−21.735	2.2294
5	−2.8362	−21.912	2.3394
6	−2.9109	−21.964	2.2943
0	−2.8955	−21.915	2.2723
M	−2.9494	−21.915	2.3106

Node *B*

EL	σ_x	σ_y	τ_{xy}
1	−3.1660	−23.866	2.9489
2	−2.0690	−22.048	1.5169
3	−3.6083	−22.257	2.0057
4	−2.3876	−19.057	1.2875
5	−3.4459	−21.476	2.5270
6	−2.1407	−21.295	2.2887
0	−3.0042	−21.796	2.1757
M	−2.8029	−21.667	2.0958

Node *C*

EL	σ_x	σ_y	τ_{xy}
1	−3.2978	−17.785	0.20719
2	−3.1446	−16.465	−0.024162
3	−3.4715	−16.548	0.025397
4	−3.0519	−15.506	−0.25193
5	−3.4652	−16.529	0.065621
6	−2.8800	−16.350	0.13921
0	−3.4722	−16.345	−0.084164
M	−3.2185	−16.530	0.025555

475 Q

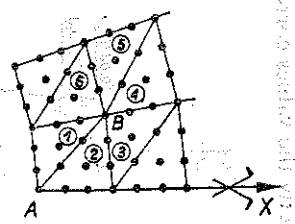

475 C

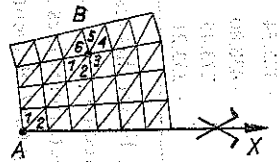

250 Q

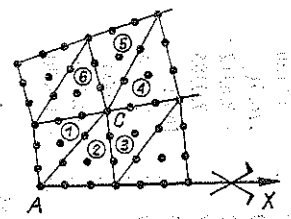

[634]

ogous values obtained by Oden's method emphasizes unimportant differences between σ_A and σ_0, e.g. in point D we have: $\sigma_A = 24.976$ and $\sigma_0 = 25.546$.

Therefore, the higher complexity of Oden's method does not seem to be rewarded by an improvement of the results as regards those provided by the simple average, at least as far as plane elasticity problems are concerned.

Nevertheless, the comparison of the various elements will be carried out with reference to the stresses obtained by Oden's method.

5. Results obtained for the stress field with the different elements

Comparison of the solutions obtained for the stress field is accomplished referring to the number of d.o.f. as well; the same structural problems assumed for displacements are considered. The accuracy of the various elements is once more discussed with reference to the mean error defined by Eq. (3.1) and to the quantities e_r and N_0 mentioned above. Approximation of the stress solutions is examined by considering the error of the principal stresses σ_I and σ_{II} which provide a global picture of the

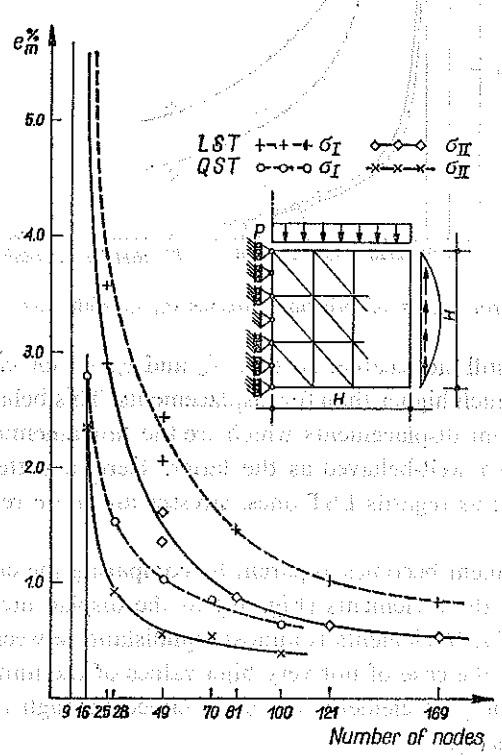

Fig. 12. *B1*: error curves of principal stresses σ_I, σ_{II} with *LST*, *QST* elements.

stress field; taking account of the results obtained a more strict comparison of the different elements is then accomplished.

Figures 12 and 13 show the curves e_m, N obtained for the two cases *B1* and *B4*. The analogy with Figs. 5 and 6 of displacement error can be noticed and the general

observations made in that case can be repeated. Nevertheless, both the accuracy of the solution and the convergence rate deteriorate significantly as regards displacements. In fact, in the same range of number N already considered, the slope of

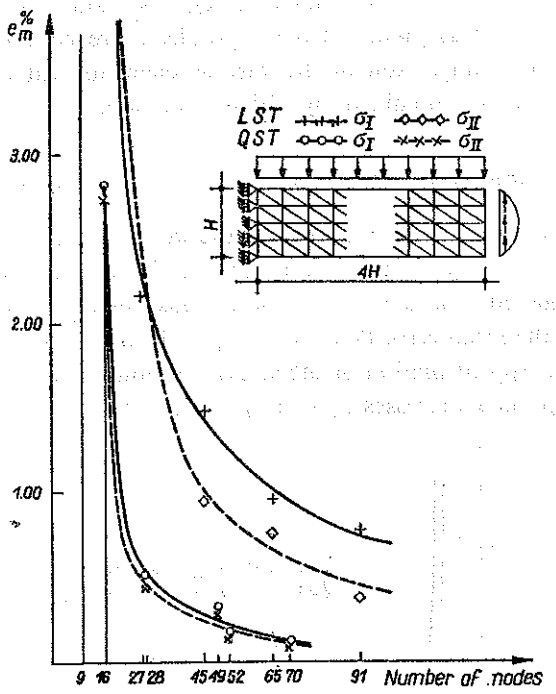

FIG. 13. *B4*: error curves of principal stresses σ_I, σ_{II} with *LST*, *QST* elements.

the stress curve is still noticeable; so that N_0 and e_r, which can be defined only approximately, are much higher than for displacements. This behaviour confirms that stresses, obtained from displacements which are the fundamental parameters of the procedure, are not so well-behaved as the latter. Here, a better accuracy of *QST* elements is obtained: as regards LST ones, stresses are more remarkably improved than displacements.

Such an improvement becomes apparent by comparing the error curves obtained for stresses with the three elements (Fig. 14) to the displacement ones (Fig. 7). In fact, the accuracy of *LST* elements is almost equidistant between those of *CST* and *QST* ones, mostly in the case of not very high values of the number of d.o.f.

Better accuracy of *QST* elements is also obtained through the analysis of more complex stress fields ([8]).

Attention is given to this subject in Table 7. The results obtained for stresses near the square plate polygonal hole confirm the equidistant position of *LST* solutions between *CST* and *QST* ones.

([8]) The diagram for case B4, analogous to the one in Fig. 14, is not reported here. A behaviour of *LST* elements nearer to *QST* ones could result from it since in this case B1 the stress field is more complex due to the greater influence of shearing forces.

Therefore, a one degree increase of the interpolation function as it occurs from a quadratic to cubic polynomial, allows for an improvement of the field variable lower than the one occurring from a linear to quadratic one. Nevertheless, a considerable

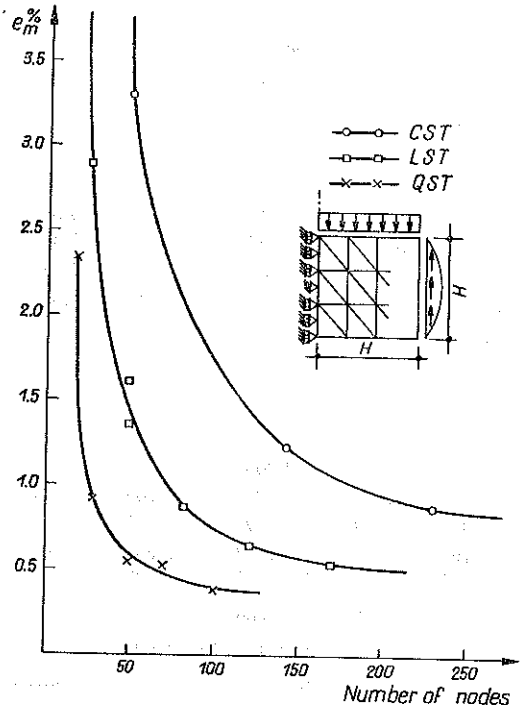

FIG. 14. $B1$: error curves of principal stress σ_{II} with the three different elements.

improvement is obtained in the approximation of the gradient of that variable: the higher it is, the greater the improvement.

Up till now, attention has been devoted to the global parameters σ_I and σ_{II} of the stress field and to their mean error. Further, the three components of the stress field and local error of the solution are carefully examined. This analysis is interesting in order to point out some features both of the procedure and of the different elements.

Table 7. Square plate: values of σ_y in point A.

Example	σ_y^A
250C	28.049
250L	28.998
250Q	30.447
475C	30.960
475L	32.131
475Q	32.570
775Q	32.986

The mean error of the components σ_x, σ_y, τ_{xy} for several solutions obtained with LST and QST elements is reported in Table 8 for $B1$ and $B4$ cases.

The error is different for the various components: higher for those with lower values and vice versa. This behaviour, which is quite interesting from the structural point of view, is connected with the variational formulation of the discretized problem; in fact, the solution error is lower just for those quantities which govern the minimization of the approximated functional and which are associated with greater energy. The above-mentionep feature of the solution

is mostly apparent in case $B4$ — the error increases considerably from σ_x to τ_{xy} and σ_y — where a remarkable difference occurs among the three stress components. On the contrary, in case $B1$, where the values of σ_x, σ_y and τ_{xy} are comparable, more uniform errors occur.

Table 8. Mean error of the stress components obtained with *LST*, *QST* elements for cases $B1$ and $B4$.

Number of nodes	$B1$		*LST*	$B4$		*LST*	Number of nodes
	σ_x	σ_y	τ_{xy}	σ_x	σ_y	τ_{xy}	
9	19.21	11.58	26.41	22.35	84.09	39.79	9
25	3.906	5.985	7.228	3.482	38.32	23.16	27
49	1.746	3.06	3.789	1.988	21.28	7.007	45
81	1.306	2.057	2.077	1.338	14.86	5.274	65
Number of nodes	$B1$		*QST*	$B4$		*QST*	Number of nodes
	σ_x	σ_y	τ_{xy}	σ_x	σ_y	τ_{xy}	
16	2.473	4.621	7.965	4.852	31.00	13.01	16
28	1.725	1.744	2.093	0.7845	9.506	3.857	28
49	1.049	1.818	1.217	0.4872	4.236	1.762	49
70	0.8816	1.368	0.7931	0.1652	1.626	0.6433	70

In terms of local results, the comparison between *LST* and *QST* elements is carried out for a discretization having the same nodes and the same element shape (Fig. 15) in case $B4$. Both mean errors of the two numerical solutions (49*L*, 49*Q*)

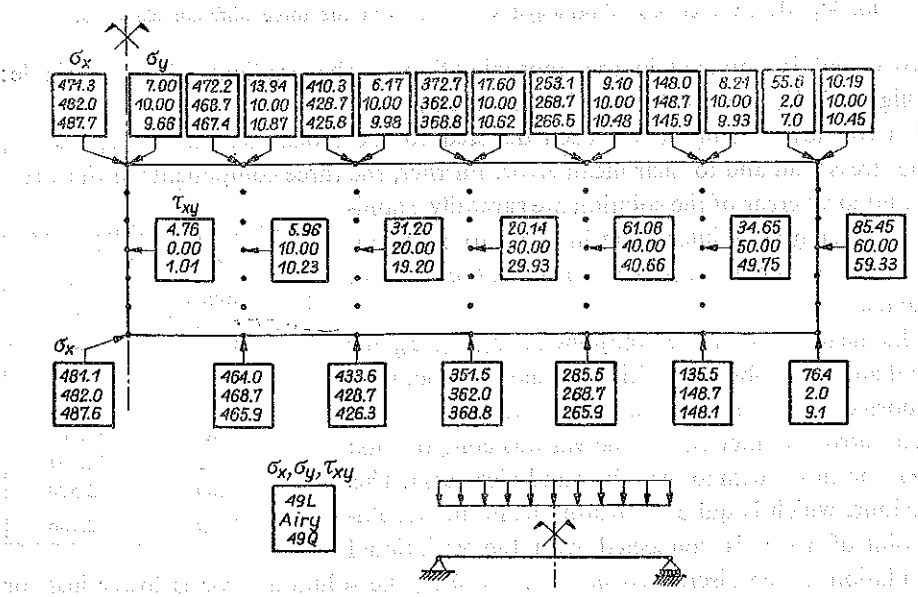

FIG. 15. $B4$: maximum values of components σ_x, σ_y, τ_{xy}. Comparison between *LST* (49 *L*) and *QST* (49 *Q*).

are very little with respect to the "exact" one (see Fig. 13). For *QST* elements, however, the local error is much more uniform with low values all over the domain; in particular, the "exact" behaviour of the components σ_y and τ_{xy} is definitely described. On the contrary, the *LST* solution is quite remote from such behaviour and shows large variations from one section to another. These results are also confirmed by comparisons carried out with a higher number of d.o.f.

Thus, *QST* elements show very little errors even for minor stress quantities, as already seen in displacement analysis, while *LST* ones penalize them. Such a behaviour, hid in the global picture via the mean error, is pointed out by error histograms, too (Fig. 16). First, attention is given to the most important component

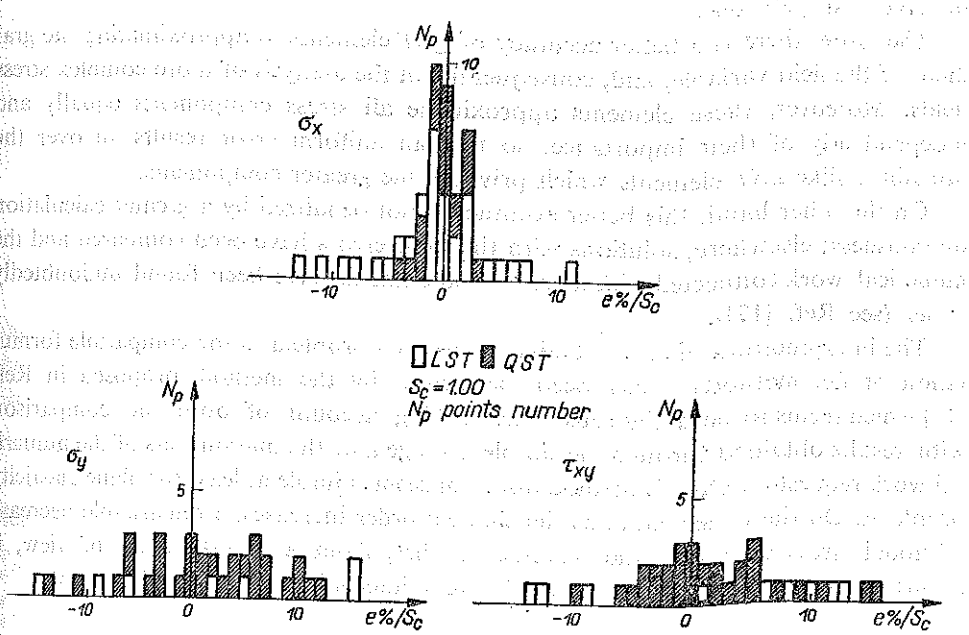

FIG. 16. Error histograms of components σ_x, σ_y, τ_{xy} for case B4. 49 nodes mesh (*LST*, *QST*).

(σ_x): both for *LST* elements and *QST* ones the results at most of the nodes are included in the range of errors considered. *QST* results are, however, more gathered around the vertical axis.

Second, if attention is paid to the other components (σ_y, τ_{xy}), the number of points included in the same range of errors is very low for *LST* elements; on the contrary, for *QST* elements only a greater scattering occurs.

The analogous histograms relative to case *B*1 confirm the behaviour already seen, even if weakened by the comparable importance of the three stress components.

6. CONCLUSIONS

In this paper a large numerical investigation has been performed to analyse the advantages connected with higher order interpolation functions in the discretization of a continuum problem into compatible finite elements.

The results confirm that accuracy improves as element order rises from linear to quadratic and cubic. Attention must be paid, however, to the features of this improvement.

The analysis of convergence properties shows that the residual error and the optimal value of the total number of nodes are always higher for *CST* elements than for *LST* and *QST* ones. Then, as far as the comparison between *LST* and *QST* elements is concerned — a problem more carefully studied in this paper — the convergence rate of the latter, as to displacements, is always more satisfactory than that of *LST* ones, while the residual errors are almost coincident. In terms of stresses, on the other hand, the behaviour of *LST* elements is nearly equidistant between those of *CST* and *QST* ones.

Therefore, there is a better accuracy of *QST* elements in approximating the gradient of the field variable, and, consequently, in the analysis of more complex stress fields. Moreover, these elements approximate all stress components equally and independently of their importance, so that an uniform error results all over the domain, unlike *LST* elements which privilege the greater components.

On the other hand, this better accuracy is not penalized by a greater calculation onerousness; elsewhere, solutions with the same errors have been compared and the numerical work connected with more refined elements have been found undoubtedly easier (see Ref. [17]).

The interpretation of stress results — always a problem in the compatible formulation of f.e. methods — has been performed by the method proposed in Ref. [12] which seems to be a rigorous one. Taking account of both the comparison with results obtained through the simple average and the onerousness of the numerical work requested, Oden's method does not seem suitable at least for plane elasticity problems. On the other hand, as the element order increases, a remarkable decrease of nodal stress discontinuities results, so that, from a general point of view, it seems not convenient to use refined stress interpolation for *QST* elements.

Appendix. Interpolation functions for Lagrangian triangular elements

In terms of areal coordinates (see Fig. 17), the interpolation functions for the elements considered in this paper are:

a) CST element:

$$n_1 = L_1, \quad n_2 = L_2, \quad n_3 = L_3;$$

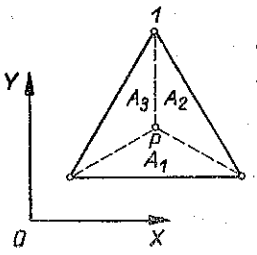

$L_1 = A_1/A \quad L_2 = A_2/A \quad L_3 = A_3/A$

$L_1 + L_2 + L_3 = 1$

b) LST element:

$$n_1 = L_1(2L_1-1), \quad n_2 = L_2(2L_2-1), \quad n_3 = L_3(2L_3-1),$$
$$n_4 = 4L_1L_2, \quad n_5 = 4L_2L_3, \quad n_6 = 4L_3L_1;$$

c) QST element:

$$n_1 = \frac{1}{2}L_1(3L_1-1)(3L_1-2), \quad n_2 = \frac{1}{2}L_2(3L_2-1)(3L_2-2),$$
$$n_3 = \frac{1}{2}L_3(3L_3-1)(3L_3-2), \quad n_4 = \frac{9}{2}L_1L_2(3L_1-1),$$
$$n_6 = \frac{9}{2}L_2L_3(3L_2-1), \quad n_8 = \frac{9}{2}L_3L_1(3L_3-1),$$
$$n_5 = \frac{9}{2}L_1L_2(3L_2-1), \quad n_7 = \frac{9}{2}L_2L_3(3L_3-1),$$
$$n_9 = \frac{9}{2}L_3L_1(3L_1-1), \quad n_{10} = 27L_1L_2L_3.$$

It is useful to obtain the interpolation functions n_i as a product of a matrix $\mathbf{B}$ having constant coefficients times a vector $\mathbf{l}_u$ depending on the areal coordinates — the order of which corresponds with $\mathbf{n}$ one and depends obviously on the element order:

(a) $$\mathbf{n} = \mathbf{B}\mathbf{l}_u.$$

Assuming the following expressions of $\mathbf{l}_u$ respectively for *CST*, *LST* and *QST* elements:

$$\mathbf{l}_u^T = \{L_1, L_2, L_3\},$$
$$\mathbf{l}_u^T = \{L_1, L_2, L_3, L_1L_2, L_2L_3, L_3L_1\},$$
$$\mathbf{l}_u^T = \{L_1, L_2, L_3, L_1L_2, L_2L_3, L_3L_1, L_1L_2^2 - L_2L_1^2, L_2L_3^2 - L_3L_2^2, L_3L_1^2 - L_1L_3^2, L_1L_2L_3\}$$

matrices $\mathbf{B}$ (see Ref. [17]) can be easily obtained.

Besides, if

$$\mathbf{I}^{-1} = \frac{1}{2A}\begin{bmatrix} y_{23} & y_{31} \\ x_{32} & x_{13} \end{bmatrix}, \qquad \mathbf{d}_l = \begin{Bmatrix} \partial/\partial L_1 \\ \partial/\partial L_2 \end{Bmatrix}$$

with $y_{23} = y_2 - y_3$, etc, there results

(b) $$\mathbf{d}_c = \mathbf{I}^{-1}\mathbf{d}_l.$$

References

1. B. Fraeijs de Veubeke, *Displacement and equilibrium models in the finite element method, Stress analysis*, O. C. Zienkiewicz, G. S. Holister [ed.], J. Wiley and son, 1965.
2. J. L. Tocher and B. J. Hartz, *Higher-order finite element for plane stress*, ASCE, J. Eng. Mech. Div. 93, EM4, 149–174, August 1967; discussion by I. Holand and P. G. Bergan, ASCE, J. Eng. Mech. Div. , 94, EM2, 698–702, April 1968.

3. P. C. DUNNE, *Complete polynomial displacement fields for finite element method*, Trans. Roy. Aero. Soc., 72, 245, 1968: discussion by B. M. IRONS, J. G. ERGATOUDIS, O. C. ZIENKIEWICZ, Trans. Roy. Aero. Soc., 72, 709–711, 1968.

4. E. R. DE ARANTES OLIVEIRA, *Theoretical foundation of the finite element method*, Int. J. Solids Struct., 4, 929–952, 1968.

5. R. S. DUNHAM and K. S. PISTER, *A finite element application of the Hellingger-Reissner variational theorem*, Proc. Conf. Matrix Meth. Struct. Mech., Wright-Patterson Air Force Base, Ohio 1968.

6. T. H. H. PIAN and P. TONG, *Basis of finite element methods for solid continua*, Intern. J. Num. Meth., 1, 3–28, 1969.

7. A. HRENNIKOFF, *Precision of finite element method in plane stress*, Pub. Int. Assn. Bridge Struct. Eng., 29-II, 125–137, 1969.

8. O. C. ZIENKIEWICZ *et al.*, *Isoparametric and associated element families for two and three-dimensional analysis*, in: *Finite element methods in stress analysis*, I. HOLAND and K. BELL [ed.], Techn. Univ. of Norway, Tapir Press, Trondheim, Norway 1969.

9. I. HOLAND, *The finite element method in plane stress analysis*, ibidem.

10. P. A. IVERSEN, *Some aspects of the finite element method in two-dimensional problems*, ibidem.

11. C. BREBBIA, *Plane stress-plane strain*, in: *Finite element techniques in structural mechanics*, H. TOTTENHAM and C. BREBBIA [ed.], Univ. of Southampton, England, 1970.

12. J. T. ODEN and H. J. BRAUCHLI, *On the calculation of consistent stress distributions in finite element approximations*, Int. J. Num. Meth. Eng., 3, 317–325, 1971.

13. J. T. ODEN and J. N. REDDY, *Note on an approximate method for computing consistent conjugate stresses in elastic finite elements*, Intern. J. Num. Meth. Eng., 6, 55–61, 1973.

14. P. PEDERSON, *Some properties of linear triangles and optimal finite element models*, Intern. J. Num. Meth. Eng., 7, 415–430, 1973.

15. D. J. TURCKE and G. M. MCNEICE, *Guidelines for selecting finite element grids based on an optimization study*, Computers and Structures, 4, 499–519, 1974.

16. G. E. RAMEY, *Some effects of system idealisations, singularities and mesh patterns on finite element solutions*, Computers and Structures, 4, 1173–1184, 1974.

17. F. BRAGA, G. REGA, F. VESTRONI, *CST, LST and QST elements in the analysis of two-dimensional elastic problems. The FINEL 1 program* (in Italian), Rep. No. 11-200, Ist. Scienza d'elle Costuzioni, Roma, 1976.

STRESZCZENIE

ANALIZA NUMERYCZNA DOSTOSOWANYCH ELEMENTÓW SKOŃCZONYCH RÓŻNEGO RZĘDU W DWUWYMIAROWYCH ZAGADNIENIACH TEORII SPRĘŻYSTOŚCI

W ostatnim dziesięcioleciu przedstawiono wiele modeli dostosowanych elementów skończonych dla płaskich zagadnień teorii sprężystości. Natomiast ilość badań teoretycznych na temat określenia efektywności różnych elementów jest nadal skąpa. Praca niniejsza dotyczy głównie porównania zachowania się dostosowanych elementów trójkątnych różnego rzędu. Porównanie przeprowadzono dla elementów *LST* i *QST* dla różnej liczby stopni swobody i dla tych zagadnień, dla których dostępne są rozwiązania analityczne. Zbieżność elementów dla aproksymacji globalnej i lokalnej rozważono oddzielnie dla pól przemieszczeń i naprężeń. Przeprowadzono również analizę numeryczną w celu porównania efektywności dwóch metod opracowanych dla zagadnień, w których występuje niejednoznaczność naprężeń w węzłach, tj. prostego uśrednienia i metody opierającej się na teorii aproksymacji sprzężonych

Резюме

ЧИСЛЕННЫЙ АНАЛИЗ ПРИСПОСОБЛЕННЫХ КОНЕЧНЫХ ЭЛЕМЕНТОВ РАЗНОГО ПОРЯДКА В ДВУМЕРНЫХ ЗАДАЧАХ ТЕОРИИ УПРУГОСТИ

В последнем десятилетии представлено много моделей приспособленных конечных элементов для плоских задач теории упругости. Вместо этого количество теоретических исследований на тему определения эффективности разных элементов в дальнейшем немногочисленно. Настоящая работа касается главным образом сравнения поведения приспособленных треугольных элементов разного порядка. Сравнение проведено для элементов *LST* и *QST* для разных значений числа степеней свободы и для таких задач, для которых доступны аналитические решения. Сходимость элементов для глобальной и локальной аппроксимации рассмотрена отдельно для полей перемещений и напряжений. Проведен тоже численный анализ с целью сравнения эффективности двух методов разработанных для задач, в которых выступает неоднозначность напряжений в узлах т.е. метода простого усреднения и метода опирающегося на теорию сопряженных аппроксимаций.

ISTITUTO DI SCIENZA DELLE COSTRUZIONI
UNIVERSITA DI ROMA

Received September 23, 1977.